A Weighted Extreme Value Moment Method Using Adaptive Sparse Grids for Time-Variant Reliability-Based Design Optimization

Hao-Ming Li, Pei-Pei Li*, and Yan-Gang Zhao
Department of Civil Engineering, Beijing University of Technology, Beijing 100124, China, lihaoming@emails.bjut.edu.cn
Department of Civil Engineering, Beijing University of Technology, Beijing 100124, China, li.peipei@bjut.edu.cn
Department of Civil Engineering, Beijing University of Technology, Beijing 100124, China, zhaoyg@bjut.edu.cn

Abstract. Time-variant reliability-based design optimization (t-RBDO) usually involves a nested-loop structure, in which repeated time-variant reliability analyses are required during design optimization. This paper proposes a weighted extreme value moment method using adaptive sparse grids for efficient t-RBDO. First, the extreme value method transforms the time-variant reliability constraints into equivalent reliability constraints based on extreme responses. The failure probability functions of the extreme responses are then constructed from their first three central moments using a three-parameter lognormal transformation. These central moment functions are obtained from raw extreme value moment functions. Next, a complete auxiliary density is introduced to express the raw moment functions as weighted integrals over the entire design domain, allowing evaluated extreme responses to be reused for different candidate designs. Subsequently, the weighted approach based on adaptive sparse grid collocation (WA-ASGC) evaluates the raw extreme value moment functions, with hierarchical surpluses guiding local refinement of the sparse grid. Finally, the resulting failure probability functions replace the time-variant probabilistic constraints, and the t-RBDO problem is solved through sequential deterministic optimization with reference point updating and local collocation point replenishment. The proposed method is non-intrusive and can be coupled with black-box numerical models. A nonlinear time-variant numerical example with two modified cases is presented to demonstrate its accuracy and efficiency.

Keywords: Time-Variant Reliability-Based Design Optimization; Extreme Value Moment; Complete Auxiliary Density; Failure Probability Function; Adaptive Sparse Grid Collocation

1. Introduction

Reliability-based design optimization (RBDO) provides a rational framework for obtaining economical designs that satisfy prescribed reliability requirements. Unlike deterministic optimization, it explicitly accounts for uncertainties in material properties, geometry, loads, and environmental actions (Valdebenito and Schueller, 2010). The most direct solution follows a double-loop structure: the outer loop searches for the optimal design, whereas the inner loop repeatedly evaluates reliability for each candidate design. Although this structure preserves the original problem formulation, a new reliability analysis is required at nearly every optimization step. The resulting cost can be prohibitive when the limit state function is nonlinear, implicit, or evaluated by finite element simulations. For time-variant RBDO (t-RBDO), each inner analysis must additionally evaluate the failure event over the design lifetime, making repeated reliability evaluation an even greater computational burden.

According to the coupling between reliability analysis and optimization, existing RBDO methods can be classified as double-loop, single-loop, and decoupled approaches. Double-loop methods are the most direct strategy. The outer loop searches for the optimal design, while the inner loop evaluates the reliability of each candidate design. The reliability index approach and performance measure approach have been developed to reduce the cost of the inner analysis (Enevoldsen and Sørensen, 1994; Ting Lin et al., 2011; Youn et al., 2005). Although the double-loop approach preserves the original reliability formulation, a new reliability analysis is still required after each design update. Single-loop methods eliminate the explicit reliability loop through optimality conditions, probabilistic transformations, or local reliability approximations. Representative developments include the adaptive hybrid single-loop method of Jiang et al. (Jiang et al., 2017) and the adaptive sampling and Kriging strategy of Zhang et al. (Zhang et al., 2021). However, these methods may depend on approximation assumptions, gradient information, or local transformations. Their application to complex nonlinear or implicit reliability problems may therefore be limited. Decoupled methods instead construct an explicit reliability function. This separates reliability analysis from optimization and avoids repeated reliability analyses during optimization.

Within decoupled RBDO, a common strategy is to construct the reliability function using surrogate models. Response surface approximations were employed by Gasser and Schueller (Gasser and Schueller, 1997) and Rajasekhar and Ellingwood (Rajasekhar and Ellingwood, 1993). Kriging or Gaussian process regression formulations were studied by Kleijnen (Kleijnen, 2009) and Zhang et al. (Zhang et al., 2022). Neural networks and polynomial chaos expansions were adopted by Papadrakakis and Lagaros (Papadrakakis and Lagaros, 2002) and Zhou et al. (Zhou and Lu, 2019; Zhou et al., 2020). These models approximate reliability-related responses or reliability functions from analyses performed at a finite number of design points. Once constructed, they avoid repeated expensive reliability analyses during optimization. However, surrogate models are fitted to limited information. They may not fully represent the true reliability mapping and may introduce additional approximation errors. Their training cost may also increase rapidly with the number of design variables. Direct construction of the failure probability function (FPF) is therefore an important decoupling strategy for RBDO.

Another class of decoupled methods directly constructs the FPF using samples or integration points generated during reliability analysis. Zou and Mahadevan (Zou and Mahadevan, 2006) used reliability sensitivity information for direct decoupling. Ching and Hsieh (Ching and Hsieh, 2007) developed a three-step method based on subset simulation. Yuan and Lu (Yuan and Lu, 2014) expressed the FPF through weighted importance samples. Subsequent developments include simulation for highly nonlinear constraints (Rashki et al., 2014), augmented line sampling (Yuan et al., 2023), stochastic subset optimization (Tafazzolis and Beck, 2009), and Markov chain Monte Carlo based decoupling (Yuan et al., 2021; Jensen et al., 2020). These methods reuse samples or response evaluations for different candidate designs. Thus, they describe the relation between the design variables and failure probability without an additional surrogate fitting process. However, an effective FPF representation over the entire design domain remains difficult, and its construction may still be computationally demanding.

More recently, two decoupled methods are particularly relevant to the present study. For t-RBDO, Zhao et al. (Zhao et al., 2023) combined an improved extreme value moment method with WA-SGNI to construct local extreme value moment and quantile functions. This approach improves the efficiency of time-variant reliability analysis. However, WA-SGNI uses a prescribed sparse grid accuracy level, and the functions are constructed in sequentially updated local design subregions. A unified representation over the entire design domain is therefore difficult to obtain. For structural RBDO, Yuan et al. (Yuan et al., 2024) proposed ASI-IS using augmented-space integration, importance sampling, subdomain updating, and sample reuse. This approach improves the efficiency of FPF estimation. However, its efficiency depends on the subdomain and sampling strategy. It also relies on failure indicators and sample weights, which may require many samples for small failure domains or strongly nonlinear limit state functions. Moreover, a common integration rule or sampling budget cannot automatically allocate computational effort according to the different refinement demands of multiple reliability constraints. Therefore, an efficient decoupled t-RBDO method that constructs the FPF over the entire design domain is still needed.

To address these issues, this paper proposes a weighted extreme value moment method using adaptive sparse grids for decoupled t-RBDO. First, the extreme value method transforms the time-variant reliability constraints into equivalent reliability constraints based on extreme responses. The failure probability functions of the extreme responses are then constructed from their first three central moments using a three-parameter lognormal transformation. These central moment functions are obtained from raw extreme value moment functions. Next, a complete auxiliary density is introduced to express the raw moment functions as weighted integrals over the entire design domain, allowing evaluated extreme responses to be reused for different candidate designs. Subsequently, WA-ASGC employs local hierarchical basis functions and surplus-guided refinement (Ma and Zabaras, 2009) to add collocation points according to the local behavior of each moment integrand. Finally, the resulting failure probability functions replace the time-variant probabilistic constraints. Sequential reference point updating and local collocation point replenishment then direct accuracy toward the candidate optimum and active reliability boundary without shrinking or relocating the prescribed design domain.

The remainder of this paper is organized as follows. Section 2 introduces the t-RBDO formulation. Section 3 presents the proposed t-RBDO methodology, including extreme value moment evaluation by WA-ASGC, moment-based failure probability transformation, and sequential deterministic optimization. Section 4 presents the numerical study, followed by the conclusions in Section 5.

2. Formulation of the t-RBDO Problem

The time-variant reliability-based design optimization (t-RBDO) problem considered in this study aims to minimize a general cost function under time-variant reliability constraints. Its formulation is given by

$$\begin{aligned}
&\text{minimize} && C(\theta) \\
&\text{subject to} && \Pr\{G_i[\mathbf{X},\mathbf{Y},\mathbf{Z}(t),t] \le 0,\ \exists t \in [0,T]\} \le P_{f_i}^t, \quad i = 1,2,\ldots,n_G, \\
& && h_j(\theta) \le 0, \quad j = 1,2,\ldots,n_h, \\
& && \underline{\theta} \le \theta \le \overline{\theta}.
\end{aligned} \tag{1}$$

where $C(\cdot)$ is the cost function; $\mathbf{X}$ is the m-dimensional design random variable vector; $\theta = [\theta_1, \theta_2, \ldots, \theta_m]^T$ is the design variable vector and consists of selected distribution parameters of $\mathbf{X}$, such as its mean values or standard deviations; $\mathbf{Y}$ is the n-dimensional classical random variable vector; and $\mathbf{Z}(t)$ is the random process vector. In addition, $G_i[\mathbf{X},\mathbf{Y},\mathbf{Z}(t),t]$ is the ith time-dependent limit state function, $P_{f_i}^t$ is the corresponding target failure probability, T is the design lifetime, $h_j(\theta)$ is the jth deterministic constraint, and $\underline{\theta}$ and $\overline{\theta}$ denote the lower and upper bounds of θ, respectively.

Based on the equivalent extreme value event, the ith time-variant reliability constraint in Eq. (1) can be expressed as

$$\Pr\{G_{ie}(\mathbf{X},\mathbf{Y},\mathbf{Z}) \le 0\} \le P_{f_i}^t, \quad i = 1,2,\ldots,n_G, \tag{2}$$

where the extreme value limit state function is defined by

$$G_{ie}(\mathbf{X},\mathbf{Y},\mathbf{Z}) = \min_{t\in[0,T]} G_i[\mathbf{X},\mathbf{Y},\mathbf{Z}(t),t]. \tag{3}$$

The random process $\mathbf{Z}(t)$ can be represented by a finite set of basic random variables and deterministic functions of time, for example through the expansion optimal linear estimation method (Zhao et al., 2023). These additional random variables can be incorporated into $\mathbf{Y}$, reducing $G_{ie}(\mathbf{X},\mathbf{Y},\mathbf{Z})$ to $G_{ie}(\mathbf{X},\mathbf{Y})$. The t-RBDO problem can therefore be rewritten as

$$\begin{aligned}
&\text{minimize} && C(\theta) \\
&\text{subject to} && \Pr\{G_{ie}(\mathbf{X},\mathbf{Y}) \le 0\} \le P_{f_i}^t, \quad i = 1,2,\ldots,n_G, \\
& && h_j(\theta) \le 0, \quad j = 1,2,\ldots,n_h, \\
& && \underline{\theta} \le \theta \le \overline{\theta}.
\end{aligned} \tag{4}$$

For the following derivation, $\mathbf{x}$ and $\mathbf{y}$ denote realizations of $\mathbf{X}$ and $\mathbf{Y}$, respectively. The density of $\mathbf{X}$ under a given design is written as $f_{\mathbf{X}}(\mathbf{x}|\theta)$, and the density of $\mathbf{Y}$ is written as $f_{\mathbf{Y}}(\mathbf{y})$. The equivalent response $G_{ie}(\mathbf{X},\mathbf{Y})$ is the extreme value of the ith limit state function over the design lifetime. Therefore, the following method constructs raw moment functions of the extreme value G_{ie}. The same construction can be applied independently to multiple reliability constraints. For a time-independent problem, the time process and the extreme value operation are omitted, and G_{ie} reduces to the ordinary limit state response.

3. Proposed t-RBDO Methodology

Section 3.1 reformulates the raw moment functions of the extreme value using the complete auxiliary density. Section 3.2 presents their numerical evaluation by WA-ASGC. Section 3.3 transforms the extreme value moments into failure probability functions. Section 3.4 details the optimization strategy.

3.1. Complete Auxiliary Density Reformulation of Extreme Value Moments

Using the equivalent extreme value response defined in Eq. (3), the kth raw moment function of the extreme value of the ith limit state function is defined as

$$m_{G_{ie}}^{k}(\theta) = E\left\{[G_{ie}(\mathbf{X},\mathbf{Y})]^k \mid \theta\right\} = \int_{\Omega_{\mathbf{x}}}\int_{\Omega_{\mathbf{y}}} G_{ie}(\mathbf{x},\mathbf{y})^k f_{\mathbf{X}}(\mathbf{x}|\theta) f_{\mathbf{Y}}(\mathbf{y})\, d\mathbf{y}\, d\mathbf{x}, \qquad k = 1,2,3. \tag{5}$$

Directly evaluating Eq. (5) at each candidate design point would still require repeated integrations over the random variable space. To obtain a reusable integral form, introduce a complete auxiliary density $h_A(\mathbf{x})$ for the design random variables (Liu et al., 2025b; Liu et al., 2025a). Multiplying and dividing the integrand in Eq. (5) by $h_A(\mathbf{x})$ gives

$$m_{G_{ie}}^{k}(\theta) = \int_{\Omega_{\mathbf{x}}}\int_{\Omega_{\mathbf{y}}} G_{ie}(\mathbf{x},\mathbf{y})^k \frac{f_{\mathbf{X}}(\mathbf{x}|\theta)}{h_A(\mathbf{x})} h_A(\mathbf{x}) f_{\mathbf{Y}}(\mathbf{y})\, d\mathbf{y}\, d\mathbf{x}, \qquad k = 1,2,3. \tag{6}$$

The complete auxiliary density is constructed from the conditional densities of $\mathbf{X}$ over the entire design domain:

$$h_A(\mathbf{x}) = \frac{1}{|\Theta|}\int_{\Theta} f_{\mathbf{X}}(\mathbf{x}|\eta)\, d\eta, \tag{7}$$

where η is an auxiliary design variable in Θ and $|\Theta|$ is the volume of the design domain. Hence, $h_A(\mathbf{x})$ is a normalized density that incorporates the random variable regions induced by all admissible design parameters.

Equivalently,

$$m_{G_{ie}}^{k}(\theta) = E_{h_A f_{\mathbf{Y}}}\left[G_{ie}(\mathbf{x},\mathbf{y})^k \frac{f_{\mathbf{X}}(\mathbf{x}|\theta)}{h_A(\mathbf{x})}\right], \qquad k = 1,2,3, \tag{8}$$

where $E_{h_A f_{\mathbf{Y}}}[\cdot]$ denotes expectation with respect to the product density $h_A(\mathbf{x}) f_{\mathbf{Y}}(\mathbf{y})$.

Eq. (6) expresses the raw moment function of the extreme value as a weighted integral under the complete auxiliary density. The extreme value response $G_{ie}(\mathbf{x},\mathbf{y})$ is evaluated at integration points governed by $h_A(\mathbf{x}) f_{\mathbf{Y}}(\mathbf{y})$, whereas the density ratio $f_{\mathbf{X}}(\mathbf{x}|\theta)/h_A(\mathbf{x})$ provides the weighting factor for each design. Thus, once these function values are available, the raw moment functions can be evaluated for different candidate designs without repeated limit state function evaluations.

3.2. WA-ASGC Evaluation of Extreme Value Moments

To evaluate Eq. (6), WA-ASGC maps the integration variable to a normalized sparse-grid space. Let $\mathbf{u} \in [-1,1]^{n_u}$ be the normalized collocation variable, and let $T(\mathbf{u}) = (\mathbf{x},\mathbf{y})$ be the corresponding physical variables. For a fixed design vector θ, the integrand of the kth raw moment of the extreme value is defined as

$$\mathcal{G}_{k\theta}(\mathbf{u}) = G_{ie}(\mathbf{x}, \mathbf{y})^k \frac{f_{\mathbf{X}}(\mathbf{x}|\theta)}{h_A(\mathbf{x})}. \tag{9}$$

Here $\mathcal{G}_{k\theta}(\mathbf{u})$ is the raw-moment integrand, $G_{ie}(\mathbf{x}, \mathbf{y})$ is the extreme value response at the transformed collocation point, $f_{\mathbf{X}}(\mathbf{x}|\theta)$ is the conditional density for a given design, and $h_A(\mathbf{x})$ is the complete auxiliary density. The notation $\mathcal{G}_{k\theta}(\mathbf{u})$ emphasizes that $\mathbf{u}$ is the integration variable, while θ is a parameter of the integrand. Substituting Eq. (9) into Eq. (6) gives

$$m^k_{G_{ie}}(\theta) = \frac{1}{2^{n_u}} \int_{[-1,1]^{n_u}} \mathcal{G}_{k\theta}(\mathbf{u})\, d\mathbf{u}, \qquad k = 1, 2, 3. \tag{10}$$

where the factor $1/2^{n_u}$ corresponds to the uniform measure on $[-1, 1]^{n_u}$.

The adaptive sparse-grid approximation is built with local hierarchical basis functions (Ma and Zabaras, 2009). The one-dimensional hat function is

$$\varphi(v) = \max(1 - |v|, 0). \tag{11}$$

For a collocation point $\mathbf{u}_p = (u_{p1}, \ldots, u_{pn_u})^T$, the corresponding multidimensional basis function is obtained by the tensor product

$$\phi_p(\mathbf{u}) = \prod_{r=1}^{n_u} \varphi\left(\frac{u_r - u_{pr}}{h_{pr}}\right). \tag{12}$$

where h_{pr} is the local support size of the basis function in the rth dimension.

Let $\mathcal{A}$ be the active sparse-grid point set. The hierarchical interpolant of $\mathcal{G}_{k\theta}$ is written as

$$A_{\mathcal{A}}(\mathcal{G}_{k\theta})(\mathbf{u}) = \sum_{p\in\mathcal{A}} c_p^{(k)}(\theta)\phi_p(\mathbf{u}). \tag{13}$$

In Eq. (13), $c_p^{(k)}(\theta)$ is the hierarchical surplus associated with point $\mathbf{u}_p$. It is defined as the difference between the actual integrand value and the previous-level prediction:

$$c_p^{(k)}(\theta) = \mathcal{G}_{k\theta}(\mathbf{u}_p) - A_{\ell_p-1}(\mathcal{G}_{k\theta})(\mathbf{u}_p). \tag{14}$$

where ℓ_p denotes the level of point $\mathbf{u}_p$, and A_{ℓ_p-1} denotes the interpolant before this point is activated.

After the interpolant is constructed, the raw moment of the extreme value is obtained by integrating the basis functions:

$$m^k_{G_{ie}}(\theta) \approx \sum_{p\in\mathcal{A}} c_p^{(k)}(\theta)\omega_p. \tag{15}$$

The coefficient ω_p in Eq. (15) is the integration weight of the basis function ϕ_p:

$$\omega_p = \frac{1}{2^{n_u}} \int_{[-1,1]^{n_u}} \phi_p(\mathbf{u})\, d\mathbf{u} = \frac{1}{2^{n_u}} \prod_{r=1}^{n_u} \int_{-1}^{1} \varphi\left(\frac{u_r - u_{pr}}{h_{pr}}\right) du_r. \tag{16}$$

The weight ω_p depends only on the sparse-grid point and the support of its basis function. The design dependence remains in $c_p^{(k)}(\theta)$ through the integrand in Eq. (9). At each collocation point, the extreme value response is evaluated once, and the values $G_{ie}(\mathbf{x},\mathbf{y})$, $G_{ie}(\mathbf{x},\mathbf{y})^2$, and $G_{ie}(\mathbf{x},\mathbf{y})^3$ are then used for the first three raw moments.

The same surplus idea is used to guide local refinement. Let $\mathcal{J}_{\theta_{\mathrm{ref}}}(\mathbf{u})$ denote the reference integrand used for refinement at the current reference design θ_{ref}. The local refinement indicator is

$$\gamma_p = \mathcal{J}_{\theta_{\mathrm{ref}}}(\mathbf{u}_p) - A_{\ell_p-1}(\mathcal{J}_{\theta_{\mathrm{ref}}})(\mathbf{u}_p). \tag{17}$$

If this indicator is larger than the prescribed tolerance ε_s, admissible neighboring points are activated:

$$|\gamma_p| > \varepsilon_s \implies \mathcal{A} \leftarrow \mathcal{A} \cup \mathcal{S}(\mathbf{u}_p), \qquad |\mathcal{S}(\mathbf{u}_p)| \leq 2n_u. \tag{18}$$

where $\mathcal{S}(\mathbf{u}_p)$ denotes the admissible neighboring points generated from $\mathbf{u}_p$. The refinement process stops when the maximum surplus over refinable active points satisfies

$$\max_{p\in\mathcal{A}_{\mathrm{ref}}} |\gamma_p| \leq \varepsilon_s. \tag{19}$$

where $\mathcal{A}_{\mathrm{ref}}$ is the set of refinable active points. Thus, new collocation points are added only in regions where the reference integrand has strong local variation. The resulting point set is then used in Eq. (15) to compute the raw moment functions of the extreme value over the design domain.

3.3. Transformation of Extreme Value Moments to the Failure Probability Function

Once the first three raw moment functions of the extreme value are known, the first three central moment functions (i.e., mean, standard deviation, and skewness) can be computed as follows:

$$\mu_{G_{ie}}(\theta) = m^1_{G_{ie}}(\theta), \tag{20a}$$

$$\sigma_{G_{ie}}(\theta) = \left[m^2_{G_{ie}}(\theta) - \left(m^1_{G_{ie}}(\theta)\right)^2\right]^{1/2}, \tag{20b}$$

$$\alpha_{3G_{ie}}(\theta) = \frac{m^3_{G_{ie}}(\theta) - 3m^2_{G_{ie}}(\theta)m^1_{G_{ie}}(\theta) + 2\left(m^1_{G_{ie}}(\theta)\right)^3}{\sigma_{G_{ie}}(\theta)^3}. \tag{20c}$$

where $\mu_{G_{ie}}(\theta)$, $\sigma_{G_{ie}}(\theta)$, and $\alpha_{3G_{ie}}(\theta)$ denote the mean value, standard deviation, and skewness of the extreme value of the ith limit state function, respectively.

For the ith reliability constraint, let $Z_i = G_{ie}(\mathbf{X},\mathbf{Y})$, with G_{ie} defined by Eq. (3), denote the extreme value response under the design vector θ, and let $F_{Z_i|\theta}(\cdot)$ be its conditional cumulative distribution function. The failure probability is

$$P_{f_i}(\theta) = \Pr\{Z_i \leq 0 \mid \theta\} = F_{Z_i|\theta}(0). \tag{21}$$

Based on the equivalent probability transformation, a response value z_i and its associated standard normal value u_i are related by equating their cumulative probabilities:

$$F_{Z_i|\theta}(z_i) = \Phi(u_i), \tag{22}$$

where $\Phi(\cdot)$ denotes the standard normal cumulative distribution function. Following the moment standardization idea, this probability-preserving relation can be written as the transformation function

$$u_i = S_i \left[z_i, \mu_{G_{ie}}(\theta), \sigma_{G_{ie}}(\theta), \alpha_{3G_{ie}}(\theta) \right]. \tag{23}$$

With the three-parameter (3P) lognormal moment transformation (Tichý, 1993), the function $S_i(\cdot)$ is written explicitly as

$$u_i = \frac{\operatorname{sign}\left[\alpha_{3G_{ie}}(\theta)\right]}{\left[\ln A(\theta)\right]^{1/2}} \ln \left\{ [A(\theta)]^{1/2} \left[1 - \frac{z_i - \mu_{G_{ie}}(\theta)}{\sigma_{G_{ie}}(\theta) u_b(\theta)} \right] \right\}. \tag{24}$$

The auxiliary quantities are

$$A(\theta) = 1 + \frac{1}{u_b(\theta)^2}, \tag{25a}$$

$$u_b(\theta) = \left[a_L(\theta) + b_L(\theta)\right]^{1/3} + \left[a_L(\theta) - b_L(\theta)\right]^{1/3} - \frac{1}{\alpha_{3G_{ie}}(\theta)}, \tag{25b}$$

$$a_L(\theta) = -\frac{1}{\alpha_{3G_{ie}}(\theta)} \left[\frac{1}{2} + \frac{1}{\alpha_{3G_{ie}}(\theta)^2} \right], \qquad b_L(\theta) = \frac{\left[\alpha_{3G_{ie}}(\theta)^2 + 4\right]^{1/2}}{2\alpha_{3G_{ie}}(\theta)^2}. \tag{25c}$$

Substituting the failure boundary $z_i = 0$ into Eq. (24) gives the standard normal value associated with failure:

$$u_{Fi}(\theta) = \frac{\operatorname{sign}\left[\alpha_{3G_{ie}}(\theta)\right]}{\left[\ln A(\theta)\right]^{1/2}} \ln \left\{ [A(\theta)]^{1/2} \left[1 + \frac{\mu_{G_{ie}}(\theta)}{\sigma_{G_{ie}}(\theta) u_b(\theta)} \right] \right\}. \tag{26}$$

The failure probability function is then obtained as

$$P_{f_i}(\theta) = \Phi\left[u_{Fi}(\theta)\right]. \tag{27}$$

For multiple reliability constraints, $P_{f_i}(\theta)$ denotes the moment-based failure probability function associated with the ith limit state function. Replacing the probabilistic constraints in Eq. (4) by Eq. (27) gives the following deterministic form:

$$\begin{aligned} \text{minimize} \quad & C(\theta) \\ \text{subject to} \quad & P_{f_i}(\theta) \le P_{f_i}^t, \quad i = 1, 2, \ldots, n_G, \\ & h_j(\theta) \le 0, \quad j = 1, 2, \ldots, n_h, \\ & \underline{\theta} \le \theta \le \overline{\theta}. \end{aligned} \tag{28}$$

Therefore, once the failure probability functions are constructed, the original reliability constraints are handled as deterministic functional constraints in the design space.

3.4. Sequential Optimization Strategy

Once the moment-based failure probability functions are available, the t-RBDO problem is solved as a sequence of deterministic optimization problems. At each iteration, after the reference point is updated, WA-ASGC recomputes the hierarchical surpluses of the current active point set for the reference integrand. If the stopping criterion in Eq. (19) is not satisfied, only admissible neighboring points generated from surplus-exceeding points according to Eq. (18) are activated and evaluated. If the criterion is already satisfied, no additional extreme value response evaluations are required.

At the rth round, the current collocation information gives $P_{f_i}^{(r)}(\theta)$, and the deterministic optimization problem is

$$\begin{aligned} \text{minimize} \quad & C(\theta) \\ \text{subject to} \quad & P_{f_i}^{(r)}(\theta) \le P_{f_i}^t, \quad i = 1, 2, \ldots, n_G, \\ & h_j(\theta) \le 0, \quad j = 1, 2, \ldots, n_h, \\ & \underline{\theta} \le \theta \le \overline{\theta}. \end{aligned} \tag{29}$$

The candidate optimum obtained from Eq. (29) is used as the reference point in the next round:

$$\theta_{\text{ref}}^{(r+1)} = \theta_{\text{opt}}^{(r)}. \tag{30}$$

WA-ASGC then rechecks the surplus criterion at the updated reference point. Additional collocation points are introduced only when the current active set no longer satisfies Eq. (19). For multiple reliability constraints, each limit state function is refined separately.

The iteration stops when

$$\frac{\left\| \theta_{\text{opt}}^{(r)} - \theta_{\text{opt}}^{(r-1)} \right\|}{\left\| \theta_{\text{opt}}^{(r-1)} \right\|} \le \varepsilon_\theta. \tag{31}$$

The complete procedure is summarized as follows:

1) *Initialization:* Specify the design domain, initial reference point, objective function, constraints, target failure probabilities, and tolerances.

2) *Raw moment evaluation:* Recheck the WA-ASGC surplus criterion at the current reference point, add admissible neighboring points only when Eq. (19) is violated, and compute the first three raw moment functions of the extreme value for each limit state function.

3) *Failure probability evaluation:* Transform the extreme value moments into $P_{f_i}^{(r)}(\theta)$.

4) *Deterministic optimization:* Solve Eq. (29) to obtain $\theta_{\text{opt}}^{(r)}$.

5) *Reference point update:* Set $\theta_{\text{ref}}^{(r+1)} = \theta_{\text{opt}}^{(r)}$.

6) *Convergence check:* Stop if Eq. (31) is satisfied; otherwise, return to Step 2.

Throughout the optimization, the complete auxiliary density and all moment integrations are defined over the same design domain Θ; no domain reduction or domain updating is required. Existing collocation points and their extreme value response values are retained, and only new points required by local refinement are added. The optimizer therefore uses deterministic failure probability functions, and any suitable optimization algorithm can be employed.

4. Numerical Study

A nonlinear time-variant numerical problem with multiple reliability constraints is used to examine the proposed method. In addition to the benchmark case, two modified cases are considered to test different feasible regions and optimum locations.

4.1. Nonlinear Time-Variant Problem

The example considers a mathematical design optimization problem adapted from the t-RBDO benchmark in (Zhao et al., 2023). It involves two normal random variables, $X_1 \sim N(\mu_1, 0.6)$ and $X_2 \sim N(\mu_2, 0.6)$, where the design variable vector is $\theta = [\mu_1, \mu_2]^T$. The t-RBDO problem is formulated as

$$\begin{aligned} &\text{minimize} && C(\theta) = \theta_1 + \theta_2 \\ &\text{subject to} && P\{G_i(X_1, X_2, t) \leq 0,\ \exists t \in [0, T]\} \leq P^t_{f_i}, \quad i = 1, 2, 3, \\ &&& 0 \leq \theta_1, \theta_2 \leq 10. \end{aligned} \tag{32}$$

The target failure probability is set as $P^t_{f_i} = 0.1$ for all three limit state functions, and the time interval is $[0, T] = [0, 5]$. The three time-variant limit state functions are

$$\begin{aligned} G_1(X_1, X_2, t) &= X_1^2 X_2 - 5X_1 t + (X_2 + 1)t^2 - a, \\ G_2(X_1, X_2, t) &= \frac{(X_1 + X_2 - 0.1t - 5)^2}{b} + \frac{(X_1 - X_2 + 0.2t - 12)^2}{120} - 1, \\ G_3(X_1, X_2, t) &= \frac{c}{(X_1 + 0.05t)^2 + 8(X_2 + 0.1t) - \sin(t) + 5} - 1. \end{aligned} \tag{33}$$

For the benchmark problem, $[a, b, c] = [20, 30, 90]$. Two modified cases are also considered: $[a, b, c] = [10, 30, 80]$ with $C(\theta) = \theta_1 - \theta_2$, and $[a, b, c] = [30, 30, 110]$ with $C(\theta) = -\theta_1 + \theta_2$. Other settings remain unchanged.

Figure 1 shows the zero-level boundaries of the three limit state functions and the resulting feasible regions. Changing the constants and objective function moves the optimum to different parts of the fixed design domain. The benchmark and modified cases therefore test whether the proposed method can identify solutions governed by different active constraints and optimum locations.

Table I compares the optimization results for the benchmark case. The proposed method gives an optimal cost of 7.7768, differing from the DL-MCS reference by approximately 0.05%, and requires 901 limit state function evaluations over four iterations. The required number of evaluations is also lower than those of WA-SGNI and ASI-IS reported in the table. Moreover, the evaluations are distributed unevenly among the three constraints: 671 for G_1, 165 for G_2, and 65 for G_3. Because each limit state function is refined independently, WA-ASGC assigns more evaluations to the more demanding moment integrand and avoids applying the same computational effort to all constraints.

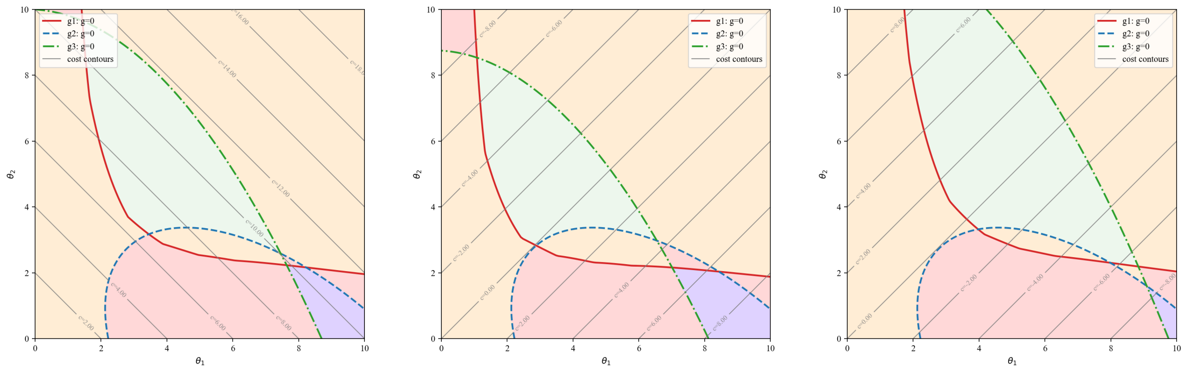

(a) Benchmark (b) Modified case 1 (c) Modified case 2

Figure 1. Limit state boundaries and optimal designs for the benchmark and modified nonlinear time-variant problems.

Table I. Results of the nonlinear time-variant problem.

Method	Optimal design point	Optimal cost	g-calls	Iterations
DL-MCS	$[3.7197, 4.0528]$	7.7726	9×10^6	9
WA-SGNI[a]	$[3.6886, 4.0836]$	7.7734	$3 \times 3 \times 135$	3
ASI-IS[b]	$[3.7834, 4.0771]$	7.8605	$4 \times (3 \times 3000)$	4
Proposed	$[3.7611, 4.0157]$	7.7768	$671 + 165 + 65$	4

[a] Ref. (Zhao et al., 2023); [b] Ref. (Yuan et al., 2024).

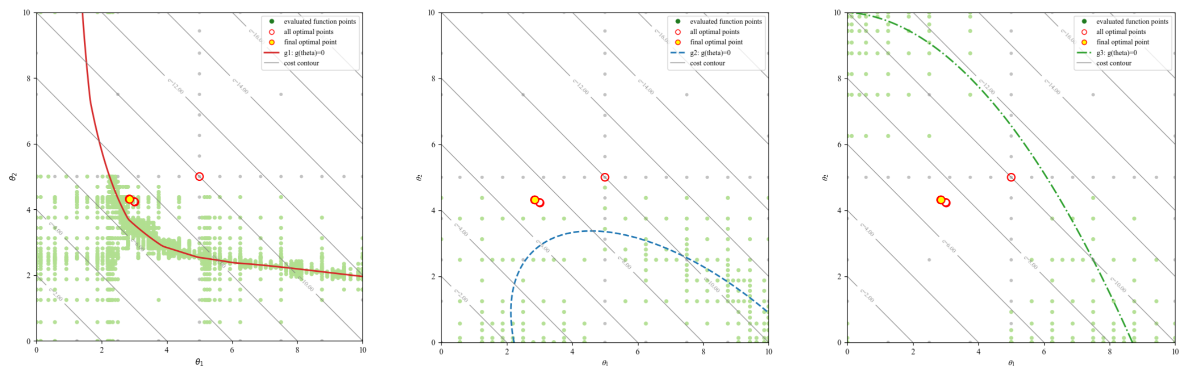

(a) g_1 (b) g_2 (c) g_3

Figure 2. Adaptive sparse grid point distributions for the benchmark nonlinear time-variant problem.

The point distributions in Fig. 2 explain this difference in computational effort. The collocation points are enriched along the relevant portions of the limit state boundaries and around the sequence of candidate optima, whereas regions with little influence on the active constraints remain sparsely represented. The different refinement patterns for G_1, G_2, and G_3 are consistent with their different numbers of function evaluations in Table I.

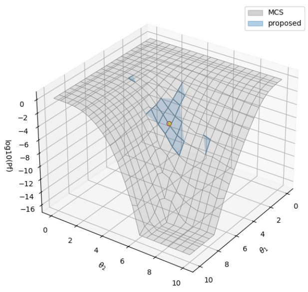

(a) Iteration 1

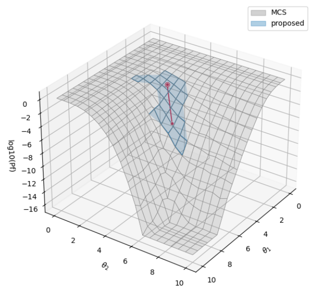

(b) Iteration 2

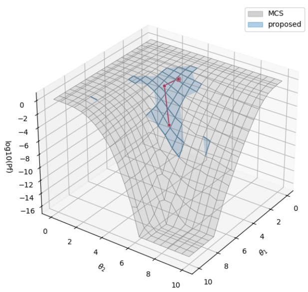

(c) Iteration 3

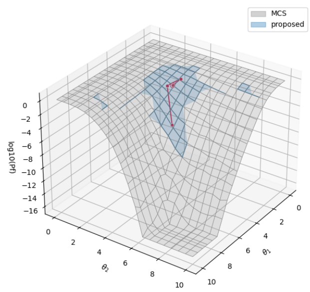

(d) Iteration 4

Figure 3. Comparative results of failure probability estimates obtained by the proposed method and MCS for the benchmark nonlinear time-variant problem.

Figure 3 compares the failure probability estimates obtained by the proposed method and MCS during the sequential optimization. Although discrepancies may remain away from the current search region, the local estimate is progressively refined as the candidate optimum is updated. At the final iteration, the two results agree closely near the optimum and the active reliability boundary. This agreement is the relevant requirement for t-RBDO and confirms that the sequential strategy directs numerical accuracy toward the region controlling the optimization solution rather than seeking uniform accuracy over the entire design domain.

Table II summarizes the results for the two modified cases.

Table II. Results of the two modified nonlinear time-variant problems.

Method	Optimal design point	Optimal cost	g-calls	Iterations
Case 1: $[a, b, c] = [10, 30, 80]$, $C(\theta) = \theta_1 - \theta_2$				
DL-MCS	$[1.9469, 7.2308]$	-5.2839	12×10^6	12
WA-SGNI[a]	$[1.9491, 7.2365]$	-5.2874	$5 \times 3 \times 135$	5
ASI-IS[b]	$[1.9671, 7.422]$	-5.4549	$5 \times (3 \times 3000)$	5
Proposed	$[1.9418, 7.2106]$	-5.2687	$496 + 131 + 256$	5
Case 2: $[a, b, c] = [30, 30, 110]$, $C(\theta) = -\theta_1 + \theta_2$				
DL-MCS	$[8.1629, 3.0658]$	-5.0971	31×10^6	31
WA-SGNI[a]	$[8.1629, 3.0647]$	-5.0982	$5 \times 3 \times 135$	5
ASI-IS[b]	$[8.1092, 2.9989]$	-5.1103	$5 \times (3 \times 3000)$	5
Proposed	$[8.1562, 3.0564]$	-5.0997	$997 + 539 + 455$	5

[a] Ref. (Zhao et al., 2023); [b] Ref. (Yuan et al., 2024).

For Cases 1 and 2, the relative differences in optimal cost from the DL-MCS references are approximately 0.29% and 0.05%, respectively. The proposed method therefore retains its accuracy when both the feasible region and the location of the optimum change. The two solutions are obtained with 883 and 1991 limit state function evaluations, respectively, without shrinking or relocating the design domain. Together with Fig. 1, these results indicate that the method can follow different active constraints and locate optima in distinct parts of the prescribed design domain while maintaining substantially lower computational cost than DL-MCS.

5. Conclusions

This paper proposed an efficient decoupled t-RBDO method based on weighted extreme value moments and adaptive sparse grids. First, the extreme value method was used to convert the time-variant reliability constraints into equivalent reliability constraints based on extreme responses. The failure probability functions of the extreme responses were then constructed from their first three central moments using the three-parameter lognormal transformation. These central moment functions were obtained from raw extreme value moment functions. Next, a complete auxiliary density was introduced to decouple reliability analysis from optimization over the prescribed design domain. Finally, WA-ASGC evaluated the raw extreme value moment functions through local refinement guided by hierarchical surpluses, thereby enabling an efficient solution of the t-RBDO problem. Based on this formulation, the main conclusions are summarized as follows:

1. A complete auxiliary density is constructed to cover the entire design domain, thereby eliminating the need for iterative domain updates during optimization.

2. A weighted adaptive sparse grid integration strategy is proposed. Hierarchical surpluses guide local refinement, enabling efficient evaluation of the extreme value moment functions and improving computational resource allocation across multiple reliability constraints.
3. A complete t-RBDO solution procedure based on weighted extreme value moments and adaptive sparse grids is established. Its accuracy in reliability analysis, computational efficiency, and applicability to complex nonlinear problems are verified through numerical examples.

Although the proposed method is computationally efficient, it still has some limitations. The method has mainly been verified for low-dimensional problems, and its applicability to problems involving complex high-dimensional random variables and large-scale finite element models requires further study. In addition, constructing the complete auxiliary density over a wide design domain may introduce additional computational cost.

Acknowledgements

The authors gratefully acknowledge the support of the National Key R&D Program of China (2023YFC3009300, 2023YFC3009302).

References

Ching, J. and Y.-H. Hsieh: 2007, 'Approximate Reliability-Based Optimization Using a Three-Step Approach Based on Subset Simulation'. *Journal of Engineering Mechanics* **133**(4), 481–493.

Enevoldsen, I. and J. D. Sørensen: 1994, 'Reliability-Based Optimization in Structural Engineering'. *Structural Safety* **15**, 169–196.

Gasser, M. and G. I. Schueller: 1997, 'Reliability-Based Optimization of Structural Systems'. *Mathematical Methods of Operations Research* **46**, 287–307.

Jensen, H., D. Jerez, and M. A. Valdebenito: 2020, 'An Adaptive Scheme for Reliability-Based Global Design Optimization: A Markov Chain Monte Carlo Approach'. *Mechanical Systems and Signal Processing* **143**, 106836.

Jiang, C., H. Liu, L. Gao, X. Cai, and P. Li: 2017, 'An Adaptive Hybrid Single-Loop Method for Reliability-Based Design Optimization Using Iterative Control Strategy'. *Structural and Multidisciplinary Optimization* **56**, 1271–1286.

Kleijnen, J. P. C.: 2009, 'Kriging Metamodeling in Simulation: A Review'. *European Journal of Operational Research* **192**, 707–716.

Liu, J., M. A. Valdebenito, D. Yang, and M. G. R. Faes: 2025a, 'Adaptive Single-Loop Reweighted Numerical Integration for Estimating Response Moment Functions Under Hybrid Aleatory and Epistemic Uncertainties'. SSRN preprint.

Liu, J., D. Yang, C. Dang, M. A. Valdebenito, and M. G. R. Faes: 2025b, 'A Single-Loop Reweighted Numerical Integration Method for Failure Probability Function Estimation Under Parametric Probability Boxes'. SSRN preprint.

Ma, X. and N. Zabaras: 2009, 'An adaptive hierarchical sparse grid collocation algorithm for the solution of stochastic differential equations'. *Journal of Computational Physics* **228**(8), 3084–3113.

Papadrakakis, M. and N. D. Lagaros: 2002, 'Reliability-Based Structural Optimization Using Neural Networks and Monte Carlo Simulation'. *Computer Methods in Applied Mechanics and Engineering* **191**, 32, 3402, 3491–3507.

Rajasekhar, R. and B. R. Ellingwood: 1993, 'A New Look at the Response Surface Approach for Reliability Analysis'. *Structural Safety* **12**, 205–220.

Rashki, M., M. Miri, and M. A. Moghaddam: 2014, 'A Simulation-Based Method for Reliability Based Design Optimization Problems with Highly Nonlinear Constraints'. *Automation in Construction* **47**, 24–36.

Tafazzolis, A. A. and J. L. Beck: 2009, 'Stochastic Subset Optimization for Reliability Optimization and Sensitivity Analysis in System Design'. *Computers & Structures* **87**, 318–331.

Tichý, M.: 1993, *Applied Methods of Structural Reliability*. Dordrecht: Kluwer Academic Publishers.

Ting Lin, P., H. Chang Gea, and Y. Jaluria: 2011, 'A Modified Reliability Index Approach for Reliability-Based Design Optimization'. *Journal of Mechanical Design* **133**, 044501.

Valdebenito, M. A. and G. I. Schueller: 2010, 'A Survey on Approaches for Reliability-Based Optimization'. *Structural and Multidisciplinary Optimization* **42**(5), 645–663.

Youn, B. D., K. K. Choi, and L. Du: 2005, 'Enriched Performance Measure Approach for Reliability-Based Design Optimization'. *AIAA Journal* **43**, 874–884.

Yuan, X., S. Liu, M. A. Valdebenito, M. G. Faes, D. Jerez, H. A. Jensen, and M. Beer: 2021, 'Decoupled Reliability-Based Design Optimization Using Markov Chain Monte Carlo in Augmented Space'. *Advances in Engineering Software* **157**, 103020.

Yuan, X. and Z. Lu: 2014, 'Efficient Approach for Reliability-Based Optimization Based on Weighted Importance Sampling Approach'. *Reliability Engineering & System Safety* **134**, 107–114.

Yuan, X., M. A. Valdebenito, B. Zhang, M. Faes, and M. Beer: 2023, 'Efficient Decoupling Approach for Reliability-Based Optimization Based on Augmented Line Sampling and Combination Algorithm'. *Computers & Structures* **280**, 107003.

Yuan, X., S. Wang, Y. Dong, and C. Yin: 2024, 'Augmented Space Integral Approach for Structural Reliability-Based Optimization'. *AIAA Journal*.

Zhang, H., D. Auex, Lemosse, and E. S. de Curci: 2021, 'A Single-Loop Approach with Adaptive Sampling and Surrogate Kriging for Reliability-Based Design Optimization'. *Engineering Optimization* **53**(8), 1450–1466.

Zhang, H., C. Zhou, H. Zhao, and Z. Zhang: 2022, 'An Ensemble Model-Based Method for Estimating Failure Probability Function with Application in Reliability-Based Optimization'. *Applied Mathematical Modelling* **108**, 445–468.

Zhao, Z., Y.-G. Zhao, and P.-P. Li: 2023, 'A Novel Decoupled Time-Variant Reliability-Based Design Optimization Approach by Improved Extreme Value Moment Method'. *Reliability Engineering & System Safety* **229**, 108825.

Zhou, Y. and Z. Lu: 2019, 'Active Polynomial Chaos Expansion for Reliability-Based Design Optimization'. *AIAA Journal* **57**, 5431–5446.

Zhou, Y., Z. Lu, and W. Yun: 2020, 'Active Sparse Polynomial Chaos Expansion for System Reliability Analysis'. *Reliability Engineering & System Safety* **202**, 107025.

Zou, T. and S. Mahadevan: 2006, 'A Direct Decoupling Approach for Efficient Reliability-Based Design Optimization'. *Structural and Multidisciplinary Optimization* **31**, 190.